Journal of Biomolecular NMR, 2 (1992) 195–202
ESCOM

J-Bio NMR 058

A refocused and optimized HNCA: Increased sensitivity and resolution in large macromolecules

B.T. Farmer II[a,*], R.A. Venters[b], L.D. Spicer[b], M.G. Wittekind[c] and L. Müller[c]

[a]*Department of Research and Development, NMR Instruments, Varian Associates, 3120 Hansen Way, Palo Alto, CA 94304, U.S.A.*
[b]*Department of Biochemistry, Duke University Medical Center, Durham, NC 27710, U.S.A.*
[c]*Bristol Myers Squibb, Pharmaceutical Research Institute, P.O. Box 4000, Princeton, NJ 08543-4000, U.S.A.*

Received 1 October 1991
Accepted 20 December 1991

Keywords: 3D NMR spectroscopy; Refocused HNCA quadruple resonance; Modified INEPT subsequence; HNC_α correlations; Synchronous ^1H broadband decoupling

SUMMARY

A 3D optimized, refocused HNCA experiment is described. It is demonstrated to yield a dramatic increase in sensitivity when applied to [^{13}C, ^{15}N]-labeled human carbonic anhydrase II, a 29-kDa protein. The reasons for the gain in sensitivity are discussed, and 3 distinct areas for further development are indicated.

A portfolio of 2D/3D {^1H, ^{13}C, ^{15}N} triple resonance experiments has recently been introduced which greatly facilitates the sequential assignment problem for large proteins (Ikura et al., 1990; Kay et al., 1990; Bax and Ikura, 1991). The weak link in several of the key experiments is the J_{NC} scalar coupling constants: $J_{NCO} \sim 15$ Hz, $J_{NC\alpha 1} \sim 11$ Hz (intraresidue), and $J_{NC\alpha 2}$ (interresidue) can be as large as 7 Hz (Bystrov, 1976; Ikura et al., 1990; Bax and Ikura, 1991). Such small values limit the size of the macromolecule to which these experiments can be applied. The HNCA experiment is undoubtedly one of the most important of the triple resonance experiments, yet suffers possibly the most in sensitivity because it makes use of the smallest of the J_{CN} scalar coupling constants. As originally pointed out (Kay et al., 1990), the HNCA experiment can in principle yield both intraresidue $H_iN_iC_{\alpha,i}$ correlations ($J_{NC\alpha 1}$) and interresidue $H_iN_iC_{\alpha,i-1}$ correlations ($J_{NC\alpha 2}$). Provided that spectral resolution is not a limiting factor, these two correlations should be sufficient to allow the sequential residue connectivity map to be constructed. In practice, many interresidue $H_iN_iC_{\alpha,i-1}$ correlations may be missing for proteins larger than 20–25 kDa, a problem

* To whom correspondence should be addressed.

0925-2738/$ 5.00

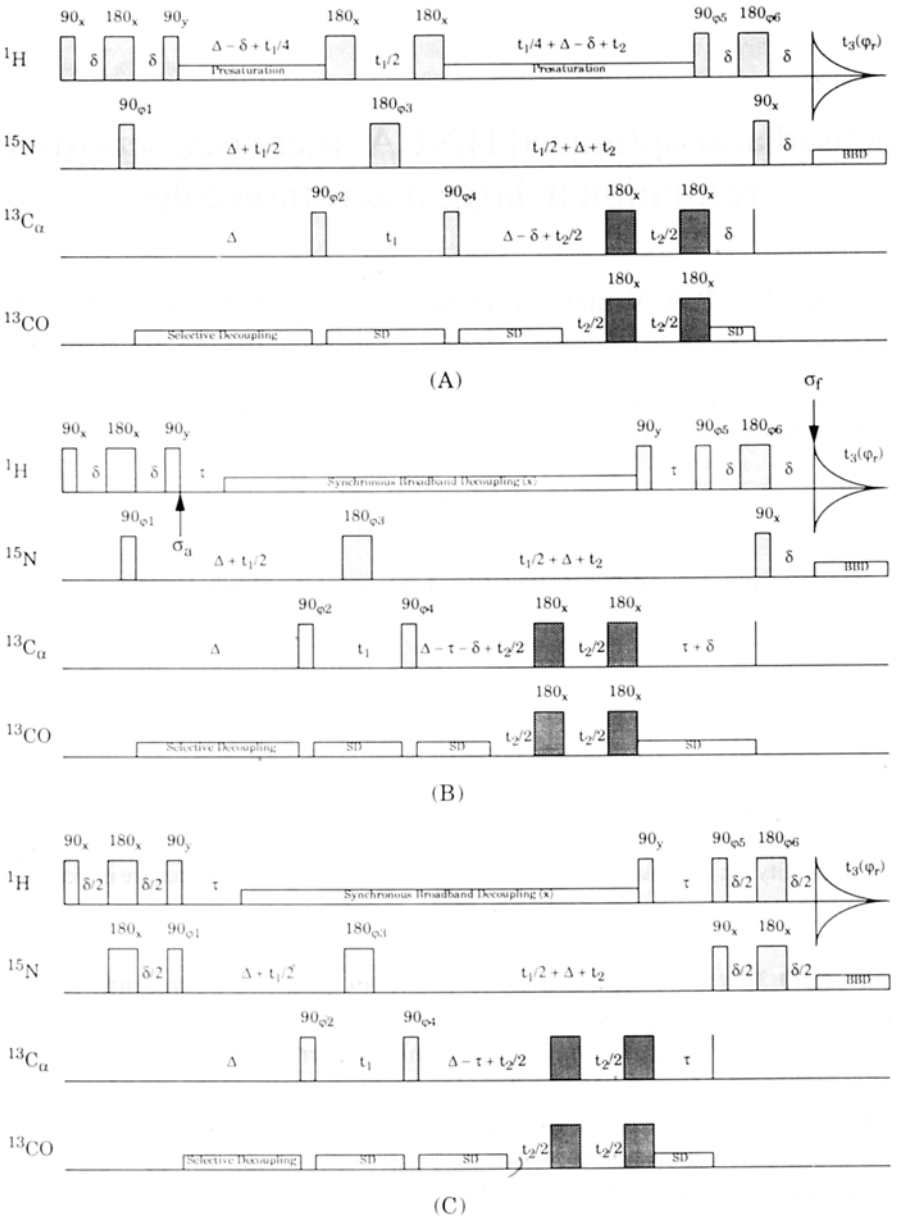

Fig. 1. Three optimized HNCA pulse sequences are presented. All ^{13}C pulses are hard, nonselective pulses. The darkly shaded 180° inversion pulses on ^{13}C during t_2 are $90_x180_y90_x$ composite pulses. BBD stands for broadband decoupling; and SD, for selective decoupling. δ is a delay optimized for both ^{15}N-^{1}H scalar interaction and ^{1}H T_2 relaxation; τ, a delay optimized solely for ^{15}N-^{1}H scalar interaction; and Δ, a delay optimized for both $^{13}C_\alpha$-^{15}N scalar interaction and ^{15}N T_2 relaxation. t_1 is the $^{13}C_\alpha$ evolution time; and t_2, the ^{15}N evolution time. The phase cycle for both of these sequences is: $\varphi_1 = 2(x), 2(-x)$; $\varphi_2 = x, -x$; $\varphi_3 = 32(x), 32(y)$; $\varphi_4 = 4(x), 4(-x)$; $\varphi_5 = 16(x), 16(-x)$; $\varphi_6 = 8(x), 8(y)$; and $\varphi_r = \varphi_1 + \varphi_2 + 2\varphi_3 + \varphi_4 + \varphi_5 + 2\varphi_6$. (A) The optimized, nonrefocused HNCA pulse sequence. (B) The optimized, refocused HNCA pulse sequence. Synchronous broadband decoupling is applied to ^{1}H for a period $\Delta - 2(\tau + \delta) + t_1 + t_2$ and is immediately followed by a 90° purge pulse, orthogonal to the effective rotation axis of the broadband decoupling sequence, as previously described (Bax et al., 1990). (C) A variant of Fig. 1B in which multiple quantum NH coherence is not created. The sensitivity relative to that for Fig. 1B is greatly influenced by T_{2MQ}/T_{2N} and T_{2MQ} (see text).

recently addressed by the HN(CO)CA experiment (Bax and Ikura, 1991). This Communication presents a general approach whereby the sensitivity of many of the triple resonance experiments can be enhanced and demonstrates the sensitivity gain in an optimized refocused 3D HNCA experiment applied to [^{13}C, ^{15}N]-labeled human carbonic anhydrase II (HCA II, ~ 29 kDa).

Four design criteria were adhered to in order to enhance the sensitivity within the HNCA experiment: (i) minimize the number of RF pulses applied to the desired quantum states; (ii) minimize the total duration of the experiment; (iii) eliminate all undesirable scalar interactions; and (iv) minimize the amount of time during which the quantum states $N^{\pm}H_z$ and $C^{\pm}N^{\pm}H_z$ exist. Figure 1A depicts a nonrefocused HNCA experiment used in assessing the gain in sensitivity offered by the refocused version. The refocused HNCA experiment, which is depicted in Fig. 1B, satisfies these 4 design criteria except that it does not eliminate the $^{13}C_{\alpha}$-$^{13}C_{\beta}$ scalar coupling interaction during t_1. The first three ^{1}H pulses and one ^{15}N pulse in Figs. 1A and B form a modified INEPT subsequence which has already been described (Farmer II, 1991). The relevant spin density matrix terms just prior to the τ delay are given by $\sigma_a(\delta)$. Using a product operator notation (Brown and Bremer, 1986) and retaining only the chemical shift and scalar coupling terms in the spin Hamiltonian,

$$\begin{aligned}\sigma_a(\delta) \propto\ & \sin(\pi J_{NH}\delta)\cos^{M-1}(\pi J_{NH}\delta)\,[4\sin(\pi J_{NC\alpha 1}\delta)\sin(\pi J_{NC\alpha 2}\delta)\,C_{\alpha 1z}C_{\alpha 2z} - \\ & 2i\sin(\pi J_{NC\alpha 1}\delta)\cos(\pi J_{NC\alpha 2}\delta)\,C_{\alpha 1z} - 2i\cos(\pi J_{NC\alpha 1}\delta)\sin(\pi J_{NC\alpha 2}\delta)\,C_{\alpha 2z}] \\ & \exp[-(\pm i\Omega_N\delta)]N^{\pm}H_z \end{aligned} \tag{1}$$

where M is the number of protons directly attached to the ^{15}N nucleus; J_{NH}, the one-bond ^{15}N-^{1}H scalar coupling constant; and Ω_N, the ^{15}N chemical shift. The effects of relaxation, resonance offset, and RF inhomogeneity are not included in Eq. 1. All backbone amides in a protein, except for the terminal amino group, are characterized by M = 1. The optimum value for δ is a function of both J_{NH} and $T_{2H(N)}$ and can be calculated from

$$\delta = (\pi J_{NH})^{-1}\tan^{-1}(\pi J_{NH}T_{2H(N)}) \tag{2}$$

where $T_{2H(N)}$ is the effective T_2 of the amide ^{1}H during the first and last δ delays. Attempts to improve the ^{15}N-^{1}H magnetization transfer efficiency in the refocused HSQC experiment (Bax et al., 1990) by using this modified INEPT subsequence have failed for HCA II (Farmer II, submitted for publication). The reason is that the modified INEPT subsequence increases the total time of the refocused HSQC pulse sequence by 2δ. Unfortunately for both HCA II and other large proteins, relaxation seems to be more detrimental to overall sensitivity than RF inhomogeneity, resonance offset, and other RF pulse imperfections in that experiment. This dilemma does not exist for the HNCA experiments depicted in Figs. 1A and B because half of the 2δ delay in each modified INEPT subsequence occurs in parallel with the Δ delay. Figure 1C presents a slight modification to Fig. 1B in that heteronuclear ^{15}N-^{1}H zero- and double-quantum coherences are never produced, albeit at a cost of two additional ^{15}N 180° inversion pulses. Neglecting any deleterious effects of RF inhomogeneity and resonance offset in these two additional ^{15}N pulses, the ratio T_{2MQ}/T_{2N} solely determines whether the pulse sequence in Fig. 1C offers any additional gain in sensitivity. The magnitude of the sensitivity difference, however, is also a function of δ/T_{2MQ} and is given by

$$\exp\{(-2\delta/T_{2MQ})(T_{2MQ}/T_{2N} - 1)\} \tag{3}$$

T_{2MQ} is the relaxation constant for the $N^{\pm}H^{\pm}$ coherence states; and T_{2N}, for single-quantum ^{15}N magnetization. One can calculate that for an amide proton in a very sparse ^{1}H environment, $T_{2MQ}/T_{2N} \sim 3$ with $\omega_N = 50$ MHz and $\tau_c = 14$ ns (Bax et al., 1990). The pulse sequence in Fig. 1B should therefore yield more sensitivity because $T_{2MQ}/T_{2N} > 1$. For an amide proton with 3 protons at 2.5 Å, 5 protons at 3.5 Å, and 7 protons at 4.5 Å, $T_{2MQ}/T_{2N} \sim 0.61$, indicating that the pulse sequence in Fig. 1C should yield more sensitivity. In the latter case, this sequence, using the experimental value of δ (see Fig. 2), should offer a maximum gain in sensitivity over the sequence in Fig. 1B of 10% for $T_{2MQ} = 40$ ms and 20% for $T_{2MQ} = 20$ ms. If each ^{15}N 180° pulse is only 95% efficient, the addition of two such pulses in Fig. 1C incurs a 10% loss in signal intensity. The question of sensitivity is therefore a complicated one and must be evaluated experimentally.

The delay τ allows the antiphase state $N^{\pm}H_z$ to refocus to the inphase state $N^{\pm}$. Because the delay τ is occurring in parallel with the delay Δ during which ^{15}N magnetization is evolving to become antiphase with respect to the C_α magnetization, the optimum value for τ is therefore a function solely of J_{NH} and is given by $1/(2J_{NH})$. It is possible for one δ delay and the τ delay to occur in parallel with the Δ delay provided that $\Delta > \delta + \tau$, which should be the case for all proteins. The optimum value for the Δ delay, during which time the $N^{\pm}C_{1\alpha,\beta}$ and $N^{\pm}C_{2\alpha,\beta}$ quantum states complete their evolution, requires a more complicated analysis. The intraresidue and interresidue NC_α magnetization transfer functions to be optimized are represented by ξ_1 and ξ_2, respectively, where

$$\xi_1 = \sin(\pi J_{NC\alpha 1}\Delta)\cos(\pi J_{NC\alpha 2}\Delta)\exp(-\Delta/T_{2Ne}) \tag{4a}$$

$$\xi_2 = \cos(\pi J_{NC\alpha 1}\Delta)\sin(\pi J_{NC\alpha 2}\Delta)\exp(-\Delta/T_{2Ne}) \tag{4b}$$

where T_{2Ne} is the effective ^{15}N T_2 relaxation time constant during the Δ delay. Calculations to determine the optimum Δ value for both the intraresidue and interresidue HNC_α correlations as a function of $J_{NC\alpha 1}$, $J_{NC\alpha 2}$, and T_{2Ne} lead to one main conclusion: the value of $J_{NC\alpha 2}$ has only a small effect on the optimum value for Δ if the T_{2Ne} values are < 20–25 ms. This conclusion greatly simplifies the problem of selecting a suitable value for Δ in the refocused HNCA experiment applied to a large protein. As an example, for $T_{2Ne} \sim 40$ ms, one should use a 21.9 ms Δ delay, which corresponds to an effective J_{CN} of 23 Hz. With this value of Δ, the intraresidue HNC_α transfer efficiency is ~ 35%; and the interresidue HNC_α transfer efficiency, ~ 20% for $J_{NC\alpha 2} = 7$ Hz.

The ratio of the intraresidue and interresidue HNC_α magnetization transfer efficiency can be estimated from

$$R_{12} = \tan^2(\pi J_{NC\alpha 1}\Delta)\cot^2(\pi J_{NC\alpha 2}\Delta) \tag{5}$$

R_{12} is evaluated to have an approximate value of 3 using the experimental value for Δ (see Fig. 2), $J_{NC\alpha 1} = 11$ Hz, and $J_{NC\alpha 2} = 7$ Hz. The intensity of each set of correlation peaks is also a function of $T_{2NC\alpha}$ and $J_{C\alpha C\beta}$. If the $T_{2NC\alpha}$ and the $J_{C\alpha C\beta}$ of both the intraresidue and the interresidue HNC_α correlation peaks are approximately the same, R_{12} should be a relatively accurate predictor for the experimental intensity ratio.

At the end of the τ delay, synchronous broadband ^{1}H decoupling, using MLEV16 (Levitt, 1986), is applied to prevent the creation of any ^{15}N-^{13}C quantum state antiphase to ^{1}H until after the ^{15}N t_2 evolution time is completed. The benefits of this are 2-fold. First, the contributions to

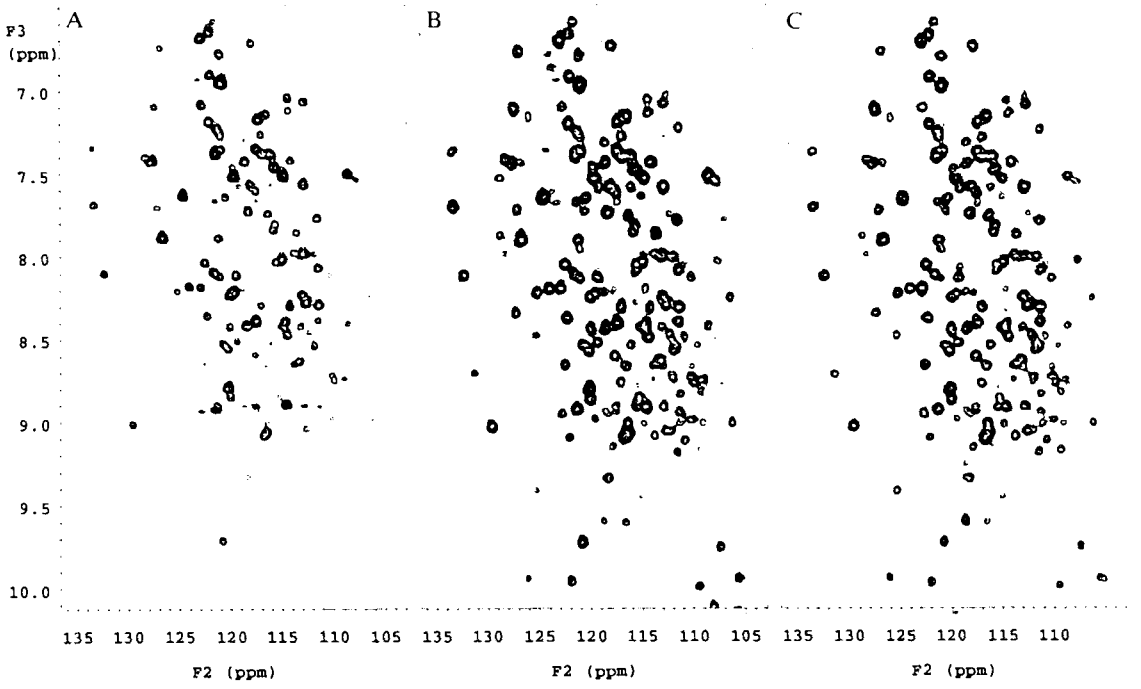

Fig. 2. 3D data from the pulse sequences in Fig. 1 applied to HCA II. The 2D ^{15}N-^{1}H skyline projection along the $^{13}C_{\alpha}$ frequency axis is presented. The sample is 1.4 mM in HCA II enriched 95% in both ^{13}C and ^{15}N. The solvent is 90% H_2O and 10% D_2O with 140 mM potassium phosphate at pH 6.5. All spectra were run at 30 C on a standard UNITY600 equipped with 3 RF channels. (A) Data acquired with the optimized, nonrefocused HNCA experiment (Fig. 1A). (B) Data acquired with the optimized, refocused HNCA experiment (Fig. 1B). (C) Data acquired with a variant of the optimized, refocused HNCA experiment (Fig. 1C). The total acquisition time for each of the 3 sequentially acquired 3D data sets is 62 h. Other pertinent acquisition parameters are: $t_{90}(^{1}H)$ = 9.5 μs, $t_{90}(^{13}C)$ = 14.8 μs, $t_{90}(^{15}N)$ = 42 μs, sw(^{1}H) = 10.0 kHz, t_1 = 51 ms, sw(^{13}C) = 3.8 kHz, t_1(max) = 8.16 ms, sw(^{15}N) = 2.3 kHz, t_2(max) = 13.5 ms, δ = 4.76 ms, τ = 5.60 ms, Δ = 16.13 ms, γB_2 = 1.25 kHz for the selective ^{13}CO decoupling, γB_1 = 4.20 kHz for the synchronous ^{1}H broadband decoupling, and γB_3 = 1.28 kHz for the broadband ^{15}N decoupling. GARP was used for the ^{15}N broadband decoupling (Shaka et al., 1985); MLEV16, for the broadband ^{1}H decoupling (Levitt, 1986); and a 25-pulse composite sequence developed by Tycko (Levitt, 1986), for the selective ^{13}CO decoupling. 64 transients were collected for each increment. The States-TPPI method was used along the t_1 and t_2 dimensions during data collection (Marion et al., 1989). The 3D data were processed on a Sun IPX to yield a final ReReRe 3D spectral data size of 64 × 128 × 1024 ($F_1F_2F_3$). No linear phase correction was required in the F_1 and F_2 spectral dimensions.

the ^{15}N and ^{13}C T_2 from ^{1}H scalar relaxation of the second kind are eliminated (Bax et al., 1990), effectively lengthening these relaxation times. As these relaxation times increase, the optimum value for Δ increases, thereby improving the overall efficiency of NC_{α} magnetization transfer. The elimination of this contribution to the ^{15}N and ^{13}C T_2 relaxation times also narrows the F_1 ^{13}C and F_2 ^{15}N linewidths as previously described in the refocused ^{15}N-^{1}H HSQC experiment (Bax et al., 1990). The decrease in linewidths leads to an increase in the 3D signal-to-noise ratio provided that there is sufficient real and/or digital resolution in these dimensions. Second, during the time in which the ^{1}H broadband decoupling is applied, $^{1}H_N$-^{1}H cross relaxation and chemical exchange

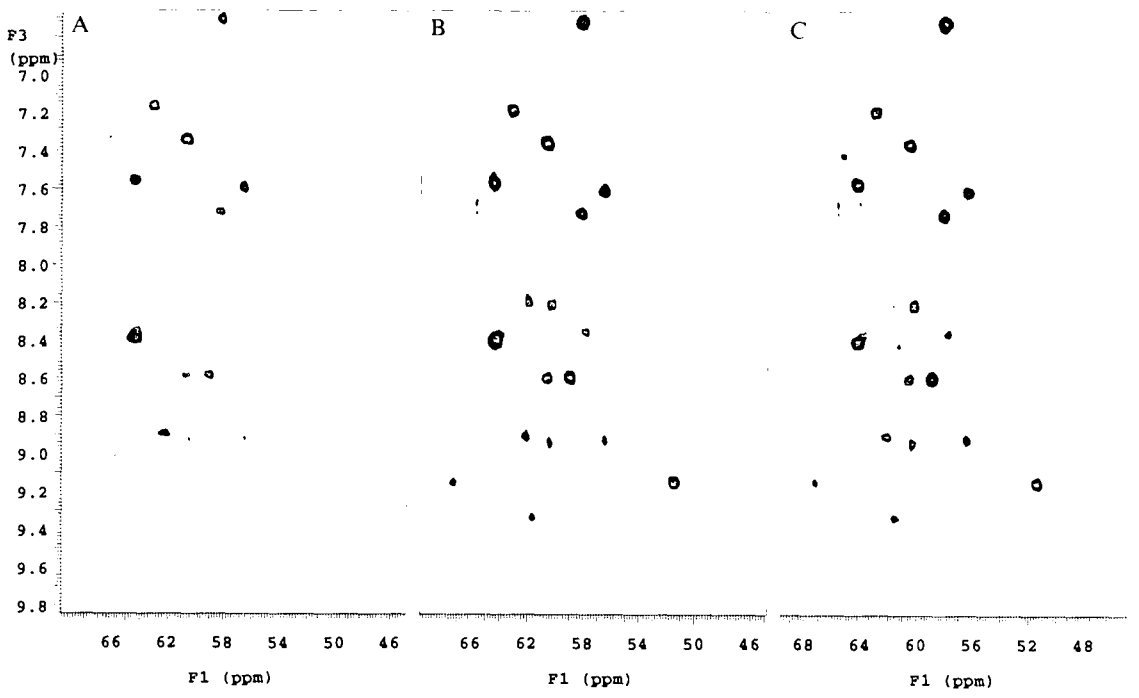

Fig. 3. 3D data from the pulse sequences in Fig. 1 applied to HCA II. The 2D ^{13}C-^{1}H plane at ^{15}N 117.66 ppm is presented. (A) Data acquired with the optimized, nonrefocused HNCA experiment (Fig. 1A). (B) Data acquired with the optimized, refocused HNCA experiment (Fig. 1B). (C) Data acquired with a variant of the optimized, refocused HNCA experiment (Fig. 1C). See the legend to Fig. 2 for details on the sample, data acquisition parameters, and relevant data processing parameters.

can not short-circuit the desired quantum states and thereby decrease the overall sensitivity of the experiment (Campbell-Burk et al., 1991).

Figures 2 and 3 display the results from the three 3D HNCA pulse sequences depicted in Fig. 1 applied to [^{13}C, ^{15}N]-labeled HCA II. Figure 2 presents the 2D ^{15}N-^{1}H skyline projection along the $^{13}C_{\alpha}$ frequency axis. Table 1 contains the volume integration for 11 correlation peaks in each of the 3 spectra in Fig. 2. These tabulated data and the qualitative appearance of the spectra in Fig. 2 support two conclusions germain to HCA II: (i) the pulse sequence described in Fig. 1A, the optimized, nonrefocused HNCA, is *clearly* inferior to either refocused HNCA sequence; and (ii) the pulse sequence described in Fig. 1B seems to yield marginally greater sensitivity over the sequence described in Fig. 1C. Figure 3 presents the ^{13}C-^{1}H 2D plane at ^{15}N 117.66 ppm. There are two sets of NC_{α} correlations which are clearly visible in Figs. 3B and C but which are either much weaker or not visible at all in Fig. 3A. The one that is not visible in Fig. 3A has correlation peaks at (^{1}H, ^{13}C) = (9.15, 67.30) and (9.15, 51.48) ppm. The one that is much weaker in Fig. 3A has correlation peaks at (^{1}H, ^{13}C) = (8.60, 60.65) and (8.60, 58.97) ppm.

Figures 2 and 3 demonstrate that the refocused HNCA experiment (Fig. 1B) can be applied to proteins as large as 29 kDa and that the gain in sensitivity over the nonrefocused experiment is significant. We have also modified the HNCO and HN(CO)CA experiments in a similar manner and are currently evaluating the performance thereof. In general, it seems to us that most of the

TABLE I
RELATIVE SENSITIVITY OF THE 3 HNCA EXPERIMENTS MEASURED BY 2D CORRELATION-PEAK VOLUME

Peak	^{1}H (ppm)	^{15}N (ppm)	A[a]	B	C
1	7.37	133.45	0.296	0.441	0.320
2	7.70	133.37	0.333	0.868	0.404
3	8.12	132.33	0.351	0.648	0.642
4	8.71	131.41	0.079	0.240	0.311
5	9.02	129.56	0.325	0.619	0.606
6	7.90	126.62	0.604	1.714	1.455
7	7.65	124.70	0.553	1.190	1.088
8	9.99	109.47	0.224	0.239	0.161
9	9.73	120.73	0.350	0.649	0.392
10	9.60	118.60	0.076	0.156	0.467
11	9.60	116.52	0.050	0.476	0.340

[a] The A–C columns contain the volume integration data from the ^{15}N-^{1}H skyline projections of the 3D data acquired with the pulse sequences in Figs. 1A–C, respectively.

published 'out-and-back' quadruple resonance experiments (Ikura et al., 1990; Kay et al., 1990; Bax and Ikura, 1991), which are *all* nonrefocused, are readily altered to accommodate ^{1}H refocusing in order to permit ^{1}H broadband decoupling during a significant portion of the entire pulse sequence.

There remain at least 4 areas in which the refocused HNCA can be improved to yield higher overall sensitivity. The first involves decoupling the C_β spins from C_α during t_1. This could be accomplished to a large degree by applying a selective 180° inversion pulse to the C_β spins. The implementation of such a selective pulse, however, would not be straightforward because there may be significant overlap between the C_α and C_β spectral regions. Moreover, the proximity of these two spectral regions would seem to rule out using selective C_β decoupling during the entire t_1 period. An alternate approach restricts the $^{13}C_\alpha$ t_1 evolution time to ~ 8 ms and uses linear prediction to extend the t_1 interferograms to longer evolution times. The second area of improvement involves using a ^{13}CO decoupling sequence more selective than the one employed to collect the data displayed in Figs. 2 and 3. The third area of improvement lies in the way that magnetization is transferred between ^{15}N and $^{13}C_\alpha$. In principle, net magnetization transfer is preferable to differential magnetization transfer in situations characterized by a small coupling constant and a large relaxation rate, e.g. the ^{15}N-$^{13}C_\alpha$ interaction in a large protein. For this reason, a biheteronuclear spin lock applied to both ^{15}N and $^{13}C_\alpha$, thereby allowing isotropic mixing to occur between these two spin types, should yield a greater efficiency in magnetization transfer, albeit at a cost of greater complexity in the pulse program and greater demands on the spectrometer hardware. Finally, it appears feasible to adapt the concept of 'constant time' (Powers et al., 1991) to the refocused HNCA experiment depicted in Fig. 1B so that the Δ delay and the t_2 evolution time occur in parallel, thereby yielding greater sensitivity. All 4 areas of improvement are currently under investigation.

ACKNOWLEDGEMENT

L.D.S. gratefully acknowledges grant support from the National Institutes of Health (R01-GM41829).

REFERENCES

Bax, A. and Ikura, M. (1991) *J. Biomol. NMR*, **1**, 99–104.
Bax, A., Ikura, M., Kay, L.E., Torchia, D.A. and Tschudin, R. (1990) *J. Magn. Reson.*, **86**, 304–318.
Brown, L.R. and Bremer, J. (1986) *J. Magn. Reson.*, **68**, 217–231.
Bystrov, V.F. (1976) *Prog. NMR Spectrosc.*, **10**, 41–81.
Campbell-Burk, S., Domaille, P. and Müller, L. (1991) *J. Magn. Reson.*, **93**, 171–177.
Farmer II, B.T. (1991) *J. Magn. Reson.*, **94**, 413–418.
Farmer II, B.T., *J. Magn. Reson.*, submitted for publication.
Ikura, M., Kay, L.E. and Bax, A. (1990) *Biochemistry*, **29**, 4659–4667.
Kay, L.E., Ikura, M., Tschudin, R. and Bax, A. (1990) *J. Magn. Reson.*, **89**, 496–514.
Levitt, M.H. (1986) *Prog. NMR Spectrosc.*, **18**, 61–122.
Marion, D., Ikura, M., Tschudin, R. and Bax, A. (1989) *J. Magn. Reson.*, **85**, 393–399.
Powers, R., Gronenborn, A.M., Clore, G.M. and Bax, A. (1991) *J. Magn. Reson.*, **94**, 209–213.
Shaka, A.J., Barker, P. and Freeman, R. (1985) *J. Magn. Reson.*, **64**, 547–552.